Classification of Psychogenic Non-epileptic Seizures Using Synchrosqueezing Transform of EEG Signals

Ozlem Karabiber Cura
Dept. of Biomedical Engineering
Izmir Katip Celebi University
Izmir, TURKEY
ozlem.karabiber@ikcu.edu.tr

Gülce Cosku Yilmaz
Dept. of Neurology,Faculty of Medicine
Izmir Katip Celebi University
Izmir, TURKEY
gulcecoskuyilmaz@gmail.com

Hatice Sabiha Türe
Dept. of Neurology,Faculty of Medicine
Izmir Katip Celebi University
Izmir, TURKEY
haticesabiha.ture@ikcu.edu.tr

Aydin Akan*
Dept. of Electrical and Electronics Eng.
Izmir University of Economics
Izmir, TURKEY
akan.aydin@ieu.edu.tr

***Abstract*—Psychogenic non-epileptic seizures (PNES) are mostly associated with psychogenic factors, where the symptoms are often confused with epilepsy. Since electroencephalography (EEG) signals maintain their normal state in PNES cases, it is not possible to diagnose using the EEG recordings alone. Therefore, long-term video EEG records and detailed patient history are needed for reliable diagnosis and correct treatment. However, the video EEG recording method is more expensive than the classical EEG. Therefore, it has great importance to distinguish PNES signals from normal epileptic seizure (ES) signals using only the EEG recordings. In the proposed study, using the Synchrosqueezed Transform (SST) that gives high-resolution time-frequency representations (TFR), inter-PNES, PNES, and Epileptic seizure EEG classification is introduced. 17 joint TF features are calculated from the TFRs, and various classifiers are used for classification processes. Classification problems with three classes (inter-PNES, PNES, and ES) and two classes (inter-PNES and PNES) are considered. Experimental results indicated that both three-class and two-class classification approaches achieved encouraging validation performances (three-class problem: 95.8% ACC, 86.9% SEN, 91.4% PRE, and 8.6% FDR; two-class problem: 96.4% ACC, 96.8% SEN, 97.3% PRE, and FDR lower than 10%).**

***Index Terms*—PNES, EEG, SST, Time-Frequency Analysis**

I. Introduction

PNES are situations that have a psychogenic origin, and resembles ES. However, electrical discharges characterized by ES are not observed in EEG patterns of the case of PNES [1], [2]. 1 out of every 4 people examined in epilepsy clinics is diagnosed with PNES, and women are 10 times more probable than men to suffer from psychogenic disorders such as PNES [3]. Although the cause of PNES is not known exactly, it is thought that many psycho-social factors and psychological mechanisms such as trauma, somatization disorder, personality factors or disorders, psychiatric comorbidity (depression, panic disorder, chronic anxiety), age factors, behavior change, gender, and psychological mechanisms may be related to PNES [4]. Many features such as stable ictal heart rate, closed eyes, pelvic thrusting, and longer-term events are more associated with PNES than ES, distinguishing ES and PNES is a challenging problem [5]. While interictal epileptiform discharges (IEDs) occur in the case of epileptic seizures, electrical activities of the brain maintain their normal state in the PNES cases. Therefore, PNES diagnosis is made base on video-EEG monitoring and patient history. However, achieving the correct diagnosis by visual examination of long-term video-EEG records is directly related to the experience of the expert neurologist, and it is a very time-consuming and tiring process. Hence, effective computer-aided diagnosis (CAD) systems are needed to accurately and quickly detect PNES cases [1], [6].

In the study [1], a method is presented for the classification of epilepsy and PNES using short-term EEG data, the functional network, and EEG sub-band features. Results of the study demonstrate that the beta-band is the most effective EEG sub-band to distinguish ES and PNES segments. In another study, common spatial pattern-based epilepsy and PNES separation is proposed. In the results of the study, accuracy of 92%, the sensitivity of 100%, the specificity of 80% values were achieved [7]. Time-frequency (TF) mapping-based epilepsy and PNES discrimination approach was performed in another study and 93% PNES detection accuracy was reported [5].

In the literature, many studies are presented to distinguish ES and PNES segments. However, since the electrical activity of the brain maintains its normal situation [1], it is difficult to distinguish the inter-PNES and PNES segments using the EEG recordings. In this paper, the high-resolution SST method-based feature extraction and classification model is proposed to distinguish ES, inter-PNES, and PNES segments. 17 joint-TF features are computed by utilizing the magnitude square of SST to capture the differences in these three classes. Various classifiers are implemented for classifying the feature set to

*This study was supported by Izmir Katip Celebi University Scientific Research Projects Coordination Unit. Project number 2019-TDR-FEBE-0005.

distinguish the PNES, inter-PNES and ES segments.

II. Materials and Methods

In this study, a novel time-frequency representation-based approach is presented to distinguish inter-PNES, PNES, and ES EEG segments. The proposed method involves obtaining joint TF representation of "inter-PNES", "PNES", and "ES" EEG segments labeled by the experts, and extracting various features from the resulting TF distributions. We propose utilizing a recently developed TF analysis method "SST" that results a close to ideal TF distribution. Joint-TF features are calculated using the energy densities obtained by SST. Finally, machine learning algorithms such as Decision tree (DT), Support Vector Machines (SVM), Random Forest (RF), and RUSBoost (RUSB) classifiers are used for the classification of generated feature sets.

A. Clinical EEG data

The dataset used in the proposed study was obtained from the Izmir Katip Celebi University School of Medicine Department of Neurology. The 18-channel EEG data were obtained from *16 epilepsy* and *6 PNES* patients, recorded using surface electrodes with 100 Hz sampling frequency. EEG signals are recorded from electrode positions of *Fp1-F7, F7-T1, T1-T3, T3-T5, T5-O1, Fp1-F3, F3-C3, C3-P3, P3-O1, Fp2-F8, F8-T2, T2-T4, T4-T6, T6-O2, Fp2-F4 F4-C4, C4-P4, P4-O2* using International 10-20 electrode placement system. However, based on expert clinician suggestions, EEG signals recorded from the temporal and frontal lobes *(Fp1-F7, F7-T1, T1-T3, T3-T5, Fp1-F3, Fp2-F8, F8-T2, T2-T4, T4-T6, Fp2-F4)* are used in the proposed study.

For the 6 PNES patients, PNES segments and inter-PNES segments are obtained based on the opinion of expert neurologist. Similarly, the ES segments are labeled and segmented for 16 epilepsy patients and used in the proposed study. Then, all inter-PNES, PNES, ES segments are divided into 1 s long segments.

B. Synchrosqueezing Transform

Synchrosqueezing Transform, a member of the family of TF reassignment methods (RM), is developed to achieve a highly localized TF representation (TFR) for non-stationary signals. SST algorithms based on both CWT and STFT have been developed in the literature, but the Fourier (STFT)-based SST approach is used in the proposed study [8]–[10]. Steps of STFT-based SST algorithm are given in the following;

1. The SST algorithm is initialized by computing the STFT "$X(\omega,t)$" of the given signal "$x(t)$".

$$X(\omega,t)=\int_{-\infty}^{\infty}x(\tau)w(\tau-t)e^{-j\omega\tau}d\tau \tag{1}$$

Here, $w(t)$ denotes the window function.

2. By calculating the derivative of "$X(\omega,t)$" with respect to time, instantaneous frequency (IF) information "$\omega_0(\omega,t)$" that is generally neglected in the STFT is achieved.

$$\omega_0(\omega,t)=Re\left(\frac{1}{2i\pi}\frac{\partial_t X(\omega,t)}{X(\omega,t)}\right) \tag{2}$$

3. Finally, the SST "$T(\eta,t)$" is obtained by utilizing IF "$\omega_0(\omega,t)$" and synchrosqueezing operator "$\int_{-\infty}^{\infty}\delta(\eta-\omega_0(\omega,t))d\omega$" [9], [10].

$$T(\eta,t)=\frac{1}{g(0)}\int_R X(\omega,t)\delta(\eta-\omega_0(\omega,t))d\omega \tag{3}$$

Examples of SST magnitude "$|T(\eta,t)|$" are demonstrated for inter-PNES, PNES, and ES EEG segments in Fig. 1.

C. Feature Extraction

The conventional time-domain or frequency-domain features or their combinations have limited performance in the analysis of non-stationary signals. Therefore, joint TF features, which are adapted versions of time- or only frequency-domain features, are computed using the resulting TFRs [11]–[13]. In the proposed study, 17 joint TF features i.e., three TF-flux, TF-flatness, TF energy concentration measure, two TF-entropy, six statistical features, five TF sub-bands energies are calculated from the TF representations of EEG signals to achieve high three-class classification performance. Joint-TF densities (TFD) "$S(n,k)''$ obtained by using magnitude square of SSTs obtained from EEG segments are used to calculate the joint TF features.

1) ***Time-frequency flux:*** This feature is calculated to measure the change of the energy of the signal in the TF domain.

$$TF_{flux}=\sum_{n=1}^{N-x}\sum_{k=1}^{M-y}|S(n+x,k+y)-S(n,k)| \tag{4}$$

Here, x and y indicate the direction of signal energy in the TF domain. In the proposed study, the three directions are take into account to calculate TF flux; for the the t axis $(x=0,y=1)$, for the f axis $(x=1,y=0)$, and for the diagonal axis $(x=1,y=1)$.

2) ***Time-frequency flatness:*** This feature is formulated by dividing the geometric mean of the TF density by its arithmetic mean.

$$F_{flat}=NM\frac{\prod_{n=1}^{N}\prod_{k=1}^{M}|S(n,k)|^{\frac{1}{NM}}}{\sum_{n=1}^{N}\sum_{k=1}^{M}S(n,k)} \tag{5}$$

3) ***Time-frequency energy concentration measure:*** This feature is computed to evaluate the concentration of signal energy in the TF domain.

$$F_{En}=(\sum_{n=1}^{N}\sum_{k=1}^{M}|S(n,k)|^{\frac{1}{2}})^2 \tag{6}$$

4) ***Time-frequency entropy:*** Joint TF normalized Renyi entropy is calculated using TFD of EEG segments.

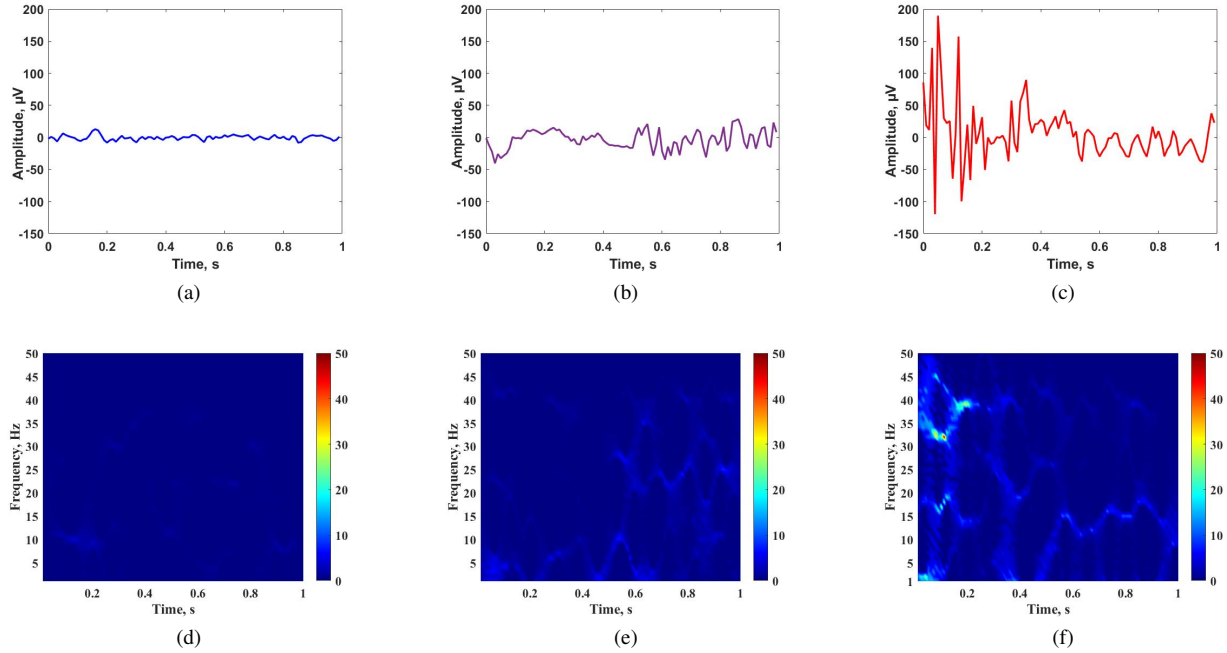

Fig. 1: 1-sec long EEG segments, (a) inter-PNES, (b) PNES, and (c) ES; magnitude SST of (d) inter-PNES, (e) PNES, and (f) ES EEG segments.

$$F_{Ren} = -\frac{1}{2}\log_2\left(\sum_{n=1}^{N}\sum_{k=1}^{M}\left(\frac{S(n,k)}{\sum_{n=1}^{N}\sum_{k=1}^{M}S(n,k)}\right)^3\right) \tag{7}$$

5) ***Statistical features:*** Six statistical features named Mean "F_{mn}", Standard deviation "F_{Sd}", Skewness F_{skew}", Kurtosis "F_{kur}", Coefficient of variation "F_{covar}", Median absolute deviation "F_{md}" are calculated using TFD.

$$F_{mn} = \mu = \frac{1}{MN}\sum_{n=1}^{N}\sum_{k=1}^{M}S(n,k)$$

$$F_{Sd} = \sigma = \sqrt{\frac{1}{MN}\sum_{n=1}^{N}\sum_{k=1}^{M}(S(n,k)-\mu)^2}$$

$$F_{skew} = \frac{1}{MN\sigma^3}\sum_{n=1}^{N}\sum_{k=1}^{M}(S(n,k)-\mu)^3$$

$$F_{kur} = \frac{1}{MN\sigma^4}\sum_{n=1}^{N}\sum_{k=1}^{M}(S(n,k)-\mu)^4$$

$$F_{covar} = \frac{\sigma}{\mu}$$

$$F_{md} = \frac{1}{MN}\sum_{n=1}^{N}\sum_{k=1}^{M}|S(n,k)-\mu| \tag{8}$$

6) ***TF sub-band energies:*** 5 joint TF sub-band energy features for $\delta : [0-4]Hz.$, $\theta : [4-8]Hz.$, $\alpha : [8-13]Hz.$, $\beta : [13-22]Hz.$, and $\gamma : [22-50]Hz.$ bands are calculated using TFDs obtained from SSTs. For example, while TF_δ denotes the joint TF energy values corresponding to δ sub-band frequencies of the TFD, TF_θ denotes the joint TF energy values corresponding to θ sub-band frequencies of the TFD.

$$TF_\delta = \sum_{n=1}^{N}\sum_{k=1}^{M_\delta}S(n,k);$$

$$TF_\theta = \sum_{n=1}^{N}\sum_{k=M_\delta+1}^{M_\theta}S(n,k)$$

$$TF_\alpha = \sum_{n=1}^{N}\sum_{k=M_\theta+1}^{M_\alpha}S(n,k);$$

$$TF_\beta = \sum_{n=1}^{N}\sum_{k=M_\alpha+1}^{M_\beta}S(n,k)$$

$$TF_\gamma = \sum_{n=1}^{N}\sum_{k=M_\beta+1}^{M}S(n,k) \tag{9}$$

D. *Classification*

In the proposed study, four classifiers; DT [14], SVM [10], RF [15], and RUSB [16] are used to classify the inter-PNES, PNES and ES segments. On account of achieving a consistent classification accuracy, $10-$ fold cross-validation is utilized in our approach. By using various statistical metrics namely, Accuracy (ACC), Sensitivity (SEN), Specificity (SPE), Preci-

sion (PRE), and False Discovery Rate (FDR), the performance evaluation of the classifiers are conducted [14], [17], [18].

$$ACC = \frac{TP+TN}{TP+FN+FP+TN}$$
$$REC = \frac{TP}{TP+FN}$$
$$SPE = \frac{TN}{FP+TN}$$
$$PRE = \frac{TP}{TP+FP}$$
$$FDR = \frac{FP}{FP+TP} \quad (10)$$

III. Experimental Results and Discussion

In this paper, the SST-based TFR approach is introduced to achieve satisfactory information for discrimination of inter-PNES, PNES, and ES EEG segments. EEG data recorded from 10 different channels of 16 epilepsy patients whose epilepsy attacks were mostly left hemisphere focused and 6 PNES patients, are examined. 1-sec long EEG segments are obtained from EEG signals of both PNES and epilepsy patients separately, and then for each EEG segment, time-frequency representations are obtained utilizing the SST approach. Using the obtained TF representations, 17 different joint TF features are computed, and 1×17 joint TF feature vector is obtained for each EEG segment.

Two cases are investigated in our study: ***(i)*** **Three-class problem:** PNES segments are identified by using the feature sets obtained from EEG segments belonging to three classes; inter-PNES, PNES, and ES. ***(ii)*** **Two-class problem:** Detecting PNES segments using two different designs; patient-dependent design (PDD), and the patient-independent design (PID), using joint TF features obtained only from the inter-PNES and PNES segments [19], [20].

1) ***Classification Results and Discussion of Three-class Problem****:* Various classifiers and different statistical performance measurement metrics are utilized to classify inter-PNES, PNES and ES EEG segments. The performance evaluation results of the proposed SST based inter-PNES, PNES and ES distinguish approach are indicated in Fig. 2. While the highest ACC, PRE, and lowest FDR are achieved using the RF classifier (ACC:95.8%, PRE:91.4%, FDR: 8.6), the highest SEN value (90.3%) is obtained using the RUSB classifier for PNES detection. Additionally, for all classifiers except SVM, higher ACC $\geq 93\%$, SEN $\geq 82\%$, and PRE $\geq 86\%$ and lower FDR $\leq 14\%$ values are obtained.

2) ***Classification Results and Discussion of Two-class problem****:* Because of interictal epileptiform discharges (IEDs) occurring in the ES, the discriminative information can be achieved between PNES and ES segments. However, the electrical activity of the brain maintains the normal situation in PNES cases. So inter-PNES and PNES distinguishing is a more challenging process for the expert neurologist. In this stage of the proposed approach, PDD and PID based PNES detection approaches are performed.

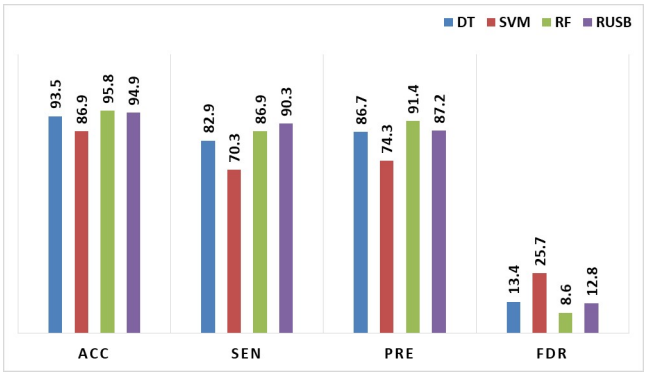

Fig. 2: Classifier based PNES detection performances.

TABLE I: Performance evaluation results of PDD based PNES detection approach (The numbers in bold represent the highest performance).

		Patient ID						
Classifiers	**Metrics**	**Pt-1**	**Pt-2**	**Pt-3**	**Pt-4**	**Pt-5**	**Pt-6**	**Avg.**
DT	**ACC**	90.8	94.2	96.1	96.6	97.6	93.3	94.77
	SEN	96	94.7	93.8	95.5	96.2	94.5	95.12
	SPE	70.1	93.8	98.4	98.1	99.1	91.6	91.85
	PRE	92.7	93.8	98.3	98.6	99.1	94.3	96.13
SVM	**ACC**	79.8	93.3	94.2	93.5	96.5	94.3	91.93
	SEN	**100**	91.4	89.4	92.5	93.7	93.2	93.37
	SPE	0	**95.2**	**99.1**	94.9	**99.5**	96	80.78
	PRE	79.8	95	**99**	96.2	**99.5**	97.2	94.45
RF	**ACC**	**92.3**	**95.2**	**97.5**	**97.3**	**98.3**	**98**	**96.43**
	SEN	96.1	95.3	**96.8**	96,6	97.8	**98.2**	**96.8**
	SPE	77.1	95.1	98.2	**98.2**	98.9	**97.7**	94.2
	PRE	94.3	**95.1**	98.2	**98.7**	99	**98.5**	**97.3**
RUSB	**ACC**	91.2	94.6	96.8	96.6	98.1	97.1	95.73
	SEN	92.5	**95.5**	96.3	**96.7**	**98.6**	97.1	96.12
	SPE	**86.5**	93.7	97.3	96.5	97.5	97.2	**94.78**
	PRE	**96.4**	93.8	97.3	97.5	98.7	98.1	96.97

Performance evaluation results of PDD based PNES detection approach are demonstrated in Table I. The highest classification accuracies are achieved with 92.3%, 95.2%, 97.5%, 97.3%, 98.3%, and 98 % using the RF classifier for six patients, respectively. While the RUSB classifier yields the maximum SEN values for Pt-1, Pt-4, and Pt-5, the highest SEN values for Pt-2 and Pt-6 are achieved using the RF classifier. However, for only Pt-1, the maximum SEN value is obtained using the SVM classifier. Additionally, while the highest average classification performance is achieved with 96.43% ACC, 96.8% SEN, 97.3% PRE values using RF classifier, the maximum average SPE value is obtained using RUSB classifier.

In addition, the performance of the PID approach is tested by creating a model with N patients minus patient-i, and the sensitivity and false discovery rate are obtained using that model when classifying an unknown patient (patient-i). Then the performance of PID and PDD-based approaches are compared for two class classification problem (given in Fig.3). To achieved average SEN and FDR values, DT, SVM, RF, and RUSB classifiers are utilized. In general, the SEN of the PDD approach is $\geq 90\%$, but the average SEN of the PID approach

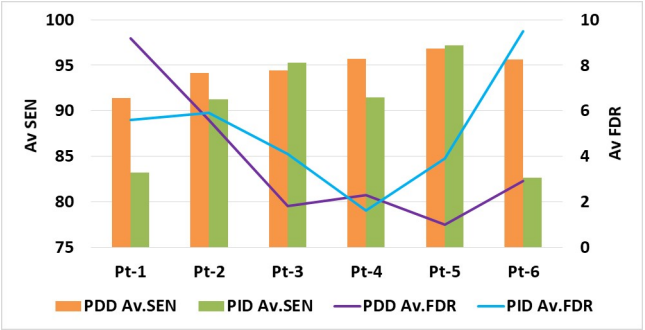

Fig. 3: Comparison of average sensitivity values and False discovery rates of PNES detection obtained by PDD and PID approaches.

for detecting unknown data is lower for some patients. For example, the average SEN values of Pt-1 and Pt-6 for the PID approach are almost 10% lower than that of the PDD approach. Additionally, both PDD and PID approaches yield lower FDR values $\leq 10\%$.

IV. Conclusion

In this paper, classification of inter-PNES, PNES, and ES EEG segments of 16 epilepsy and 6 PNES patients are investigated. By using Synchrosqueezed Transform that gives highly localized TFDs, joint TFRs of each EEG segment of PNES and epilepsy patients are obtained to achieve distinctive information between different patient groups. Joint TF features that are adapted versions of time- or frequency-domain features are calculated from TFRs and the classification processes are performed using various classifiers. Both three-class classification problem including classification of inter-PNES, PNES, and ES EEG segments, and two-class problem considering inter-PNES, PNES EEG segments are conducted. For both three-class and two-class classification problems, outstanding classification performances are achieved. In the later stages of the proposed study, it is aimed to include different features, and perform the classification using different classifiers.

References

[1] N. Ahmadi, Y. Pei, E. Carrette, A. P. Aldenkamp, and M. Pechenizkiy, "EEG-based classification of epilepsy and PNES: EEG microstate and functional brain network features," *Brain informatics*, vol. 7, pp. 1–22, 2020.

[2] E. Pippa, E. I. Zacharaki, I. Mporas, V. Tsirka, M. P. Richardson, M. Koutroumanidis, and V. Megalooikonomou, "Improving classification of epileptic and non-epileptic EEG events by feature selection," *Neurocomputing*, vol. 171, pp. 576–585, 2016.

[3] M. Oto, P. Conway, A. McGonigal, A. Russell, and R. Duncan, "Gender differences in psychogenic non-epileptic seizures," *Seizure*, vol. 14, no. 1, pp. 33–39, 2005.

[4] N. Bodde, J. Brooks, G. Baker, P. Boon, J. Hendriksen, O. Mulder, and A. Aldenkamp, "Psychogenic non-epileptic seizures—definition, etiology, treatment and prognostic issues: a critical review," *Seizure*, vol. 18, no. 8, pp. 543–553, 2009.

[5] J. Bayly, J. Carino, S. Petrovski, M. Smit, D. A. Fernando, A. Vinton, B. Yan, J. R. Gubbi, M. S. Palaniswami, and T. J. O'Brien, "Time-frequency mapping of the rhythmic limb movements distinguishes convulsive epileptic from psychogenic nonepileptic seizures," *Epilepsia*, vol. 54, no. 8, pp. 1402–1408, 2013.

[6] D. H. Toffa, L. Poirier, and D. K. Nguyen, "The first-line management of psychogenic non-epileptic seizures (pnes) in adults in the emergency: a practical approach," *Acta Epileptologica*, vol. 2, pp. 1–11, 2020.

[7] P. Xu, X. Xiong, Q. Xue, P. Li, R. Zhang, Z. Wang, P. A. Valdes-Sosa, Y. Wang, and D. Yao, "Differentiating between psychogenic nonepileptic seizures and epilepsy based on common spatial pattern of weighted EEG resting networks," *IEEE Transactions on Biomedical Engineering*, vol. 61, no. 6, pp. 1747–1755, 2014.

[8] G. Yu, M. Yu, and C. Xu, "Synchroextracting transform," *IEEE Transactions on Industrial Electronics*, vol. 64, no. 10, pp. 8042–8054, 2017.

[9] T. Oberlin, S. Meignen, and V. Perrier, "The fourier-based synchrosqueezing transform," in *2014 IEEE International Conference on Acoustics, Speech and Signal Processing (ICASSP)*, 2014, pp. 315–319.

[10] S. Mamli and H. Kalbkhani, "Gray-level co-occurrence matrix of fourier synchro-squeezed transform for epileptic seizure detection," *Biocybernetics and Biomedical Engineering*, vol. 39, no. 1, pp. 87–99, 2019.

[11] N. A. Khan and S. Ali, "A new feature for the classification of non-stationary signals based on the direction of signal energy in the time–frequency domain," *Computers in biology and medicine*, vol. 100, pp. 10–16, 2018.

[12] L. Boubchir, S. Al-Maadeed, and A. Bouridane, "On the use of time-frequency features for detecting and classifying epileptic seizure activities in non-stationary EEG signals," in *2014 IEEE International Conference on Acoustics, Speech and Signal Processing (ICASSP)*. IEEE, 2014, pp. 5889–5893.

[13] B. Boashash and S. Ouelha, "Automatic signal abnormality detection using time-frequency features and machine learning: A newborn EEG seizure case study," *Knowledge-Based Systems*, vol. 106, pp. 38–50, 2016.

[14] A. T. Tzallas, M. G. Tsipouras, and D. I. Fotiadis, "Epileptic seizure detection in EEGs using time–frequency analysis," *IEEE transactions on information technology in biomedicine*, vol. 13, no. 5, pp. 703–710, 2009.

[15] E. Alickovic, J. Kevric, and A. Subasi, "Performance evaluation of empirical mode decomposition, discrete wavelet transform, and wavelet packed decomposition for automated epileptic seizure detection and prediction," *Biomedical signal processing and control*, vol. 39, pp. 94–102, 2018.

[16] C. Seiffert, T. M. Khoshgoftaar, J. Van Hulse, and A. Napolitano, "RUSBoost: Improving classification performance when training data is skewed," in *2008 19th International Conference on Pattern Recognition*. IEEE, 2008, pp. 1–4.

[17] J. Maroco, D. Silva, A. Rodrigues, M. Guerreiro, I. Santana, and A. de Mendonça, "Data mining methods in the prediction of dementia: A real-data comparison of the accuracy, sensitivity and specificity of linear discriminant analysis, logistic regression, neural networks, support vector machines, classification trees and random forests," *BMC research notes*, vol. 4, no. 1, p. 299, 2011.

[18] S. Siuly and Y. Li, "Designing a robust feature extraction method based on optimum allocation and principal component analysis for epileptic EEG signal classification," *Computer Methods and Programs in Biomedicine*, vol. 119, no. 1, pp. 29 – 42, 2015. [Online]. Available: http://www.sciencedirect.com/science/article/pii/S0169260715000206

[19] L. A. Moctezuma and M. Molinas, "Classification of low-density EEG for epileptic seizures by energy and fractal features based on emd," *The Journal of Biomedical Research*, vol. 34, no. 3, pp. 180–190, 2020.

[20] M. Islam, T. Tanaka, Y. Iimura, T. Mitsuhashi, H. Sugano, D. Wang, M. Molla, K. Islam *et al.*, "Statistical features in high-frequency bands of interictal iEEG work efficiently in identifying the seizure onset zone in patients with focal epilepsy," *Entropy*, vol. 22, no. 12, p. 1415, 2020.